

COMPUTATION OF ZOLOTAREV RATIONAL FUNCTIONS *

LLOYD N. TREFETHEN[†] AND HEATHER D. WILBER[‡]

Abstract. An algorithm is presented to compute Zolotarev rational functions, that is, rational functions r_n^* of a given degree that are as small as possible on one set $E \subseteq \mathbb{C} \cup \{\infty\}$ relative to their size on another set $F \subseteq \mathbb{C} \cup \{\infty\}$ (the third Zolotarev problem). Along the way we also approximate the sign function relative to E and F (the fourth Zolotarev problem).

Key words. rational approximation, Zolotarev ratio problem, Zolotarev sign problem, AAA algorithm

MSC codes. 30E10, 41A20, 65D15

1. Introduction. Figures 1–3 show 14 examples of computed Zolotarev rational functions. The aim of this paper is to present the mathematics of these functions, explain why they are of interest, and show how they can be computed numerically by an algorithm combining AAA-Lawson rational approximation [23] with the equivalence of the third and fourth Zolotarev problems of classical approximation theory [17]. Each of the images in the figures was computed in a fraction of a second on a laptop. A reliable method for computing these functions has not been available before.

Let E and F be disjoint closed sets in the complex plane. For simplicity we assume that E and F each consist of one or a finite number of continua, such as arcs or domains bounded by arcs. They should be closed and disjoint in the extended complex plane $\mathbb{C} \cup \{\infty\}$, which implies that if ∞ belongs to one of the sets, it does not belong to the other.

For an integer $n \geq 0$, let R_n be the set of rational functions of degree n , which means that any $r \in R_n$ can be written as p/q for some polynomials p and q of degree at most n . The problem we are concerned with is to find a function $r_n^* \in R_n$ that minimizes the ratio

$$(1.1) \quad \frac{\max_{z \in E} |r(z)|}{\min_{z \in F} |r(z)|}.$$

Since multiplying r by a constant does not change the ratio, we may normalize the problem by fixing

$$(1.2) \quad \min_{z \in F} |r(z)| = 1.$$

This gives us what is called the third Zolotarev problem, which might also be called the *Zolotarev ratio problem*.

Problem Z3 = Zolotarev ratio problem. Find $r_n^* \in R_n$ with $\min_{z \in F} |r_n^*(z)| = 1$ that attains the minimum

$$(1.3) \quad \sigma_n = \min_r \|r\|_E,$$

*Submitted to the editors DATE. The work of the second author was supported by the National Science Foundation under Grant No. DMS-2410045.

[†]School of Engineering and Applied Sciences, Harvard University, Cambridge, MA 02138, USA (trefethen@seas.harvard.edu)

[‡]Dept. of Applied Mathematics, University of Washington, Seattle, WA 98195, USA (hdw27@uw.edu)

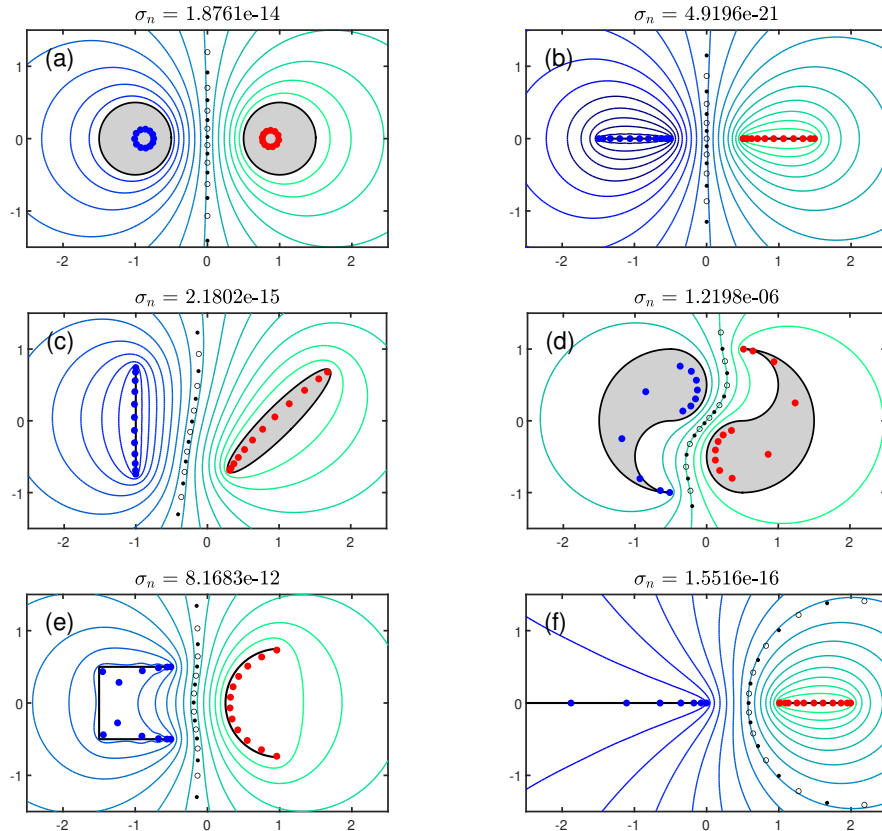


FIG. 1. Six examples of degree $n = 12$ Zolotarev rational functions r_n^* defined by connected sets E (on the left in each image) and F (on the right). The solutions plotted are near-optimal but not exactly so. The Zolotarev function r_n^* satisfies $|r_n^*(z)| \approx \min_{t \in F} |r_n^*(t)| = 1$ for z on the boundary of F , and contours show levels $\log_{10} |r_n^*(z)| = -1, -2, \dots$ between the two domains. Blue dots mark the zeros of r_n^* and red dots mark the poles. Black circles and dots mark zeros and poles of the sign function \hat{r}_n to be introduced in section 2. The minimum values $\sigma_n = \|r_n^*\|_E$ are listed in the titles. Details of the geometries are given in the appendix.

where $\|\cdot\|_E$ denotes the supremum norm over E .

It is known that a solution r_n^* to (1.3) exists, though it need not be unique, and that σ_n satisfies $0 < \sigma_n \leq 1$.

Note that there is a certain asymmetry in the normalization (1.2), which results in an asymmetry in the contour lines of Figs. 1–3. The symmetrical choice would be to scale r so that the numerator and denominator of (1.1) are reciprocals of each other. On the other hand (1.2) is standard, and algebraically simple.

We will say a few words about Figures 1–3 here, then turn in section 2 to the mathematical basis of this subject, the connection between the third and fourth Zolotarev problems of rational approximation theory. Section 3 presents our algorithm, which is based on AAA-Lawson approximation [22] enhanced by recent modifications for dealing with functions of the flavor of $f(z) = \text{sign}(z)$ and for ensuring convergence of the Lawson phase. Sections 4 and 5 discuss applications. Section 6 finishes with a few closing remarks.

Figures 1–3 differ in topology, but all show the same mathematics. In each case a

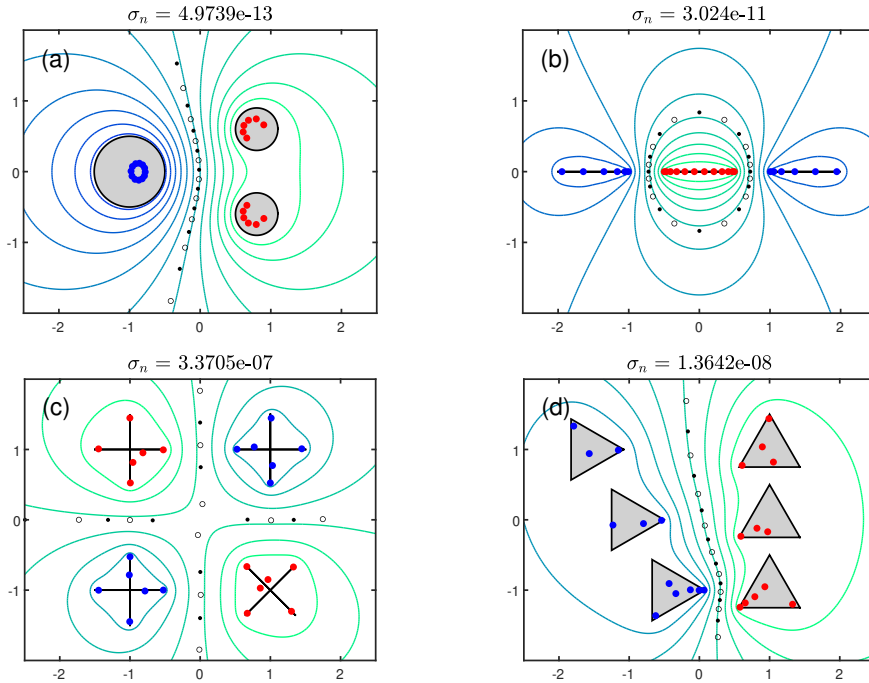


FIG. 2. The same as in Figure 1, now for four problems where E and/or F are disconnected.

close approximation to the optimal function r_n^* with $n = 12$ has been computed and is depicted by means of its zeros (blue dots), poles (red dots), and level contours

$$(1.4) \quad \log_{10} |r_n^*(z)| = -1, -2, \dots,$$

or in the case of Figure 3,

$$(1.5) \quad \log_{10} |r_n^*(z)| = -1/3, -2/3, \dots$$

The domain F can be recognized as the one containing red poles and enclosed by green contours. Because of the normalization (1.2), the zero contour $\log_{10} |r_n^*(z)| = 0$ would enclose F while just touching it; in practice this contour is very close to the boundary of F (the “near-circularity phenomenon” [30]). The levels in the plots go down as far as possible while remaining greater than $\log_{10} \sigma_n$, implying that they all enclose E , which can be recognized as the region containing blue zeros and enclosed by blue contours. The colors correspond to the same levels in all the images of Figures 1 and 2, and likewise divided by 3 in the images of Figure 3.

Each image also shows a chain of black circles and dots, representing the zeros and poles of the rational function \hat{r}_n of the fourth Zolotarev problem, as we will explain in section 2. Note that about half of our sets E and F have interiors, shaded in grey in the figures, but our calculations just sample them on the boundaries.

Looking qualitatively at the figures, we note that smaller values of σ_n correspond to cases where E and F are well separated. Thus Figure 1b, with two well separated intervals, gives $\sigma_n \approx 10^{-20}$, whereas Figure 1d, where the yin and yang are interleaved, gives $\sigma_n \approx 10^{-6}$. In the examples of Figure 3, E is wholly enclosed by F , and the values of σ_n are closer to 1.

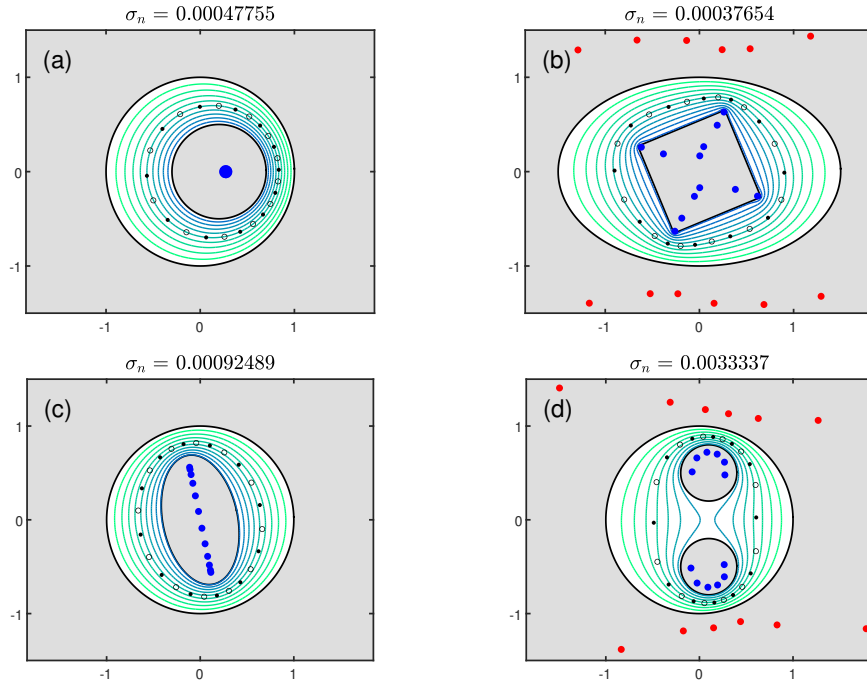


FIG. 3. The same as in Figures 1 and 2, now for domains where F encloses E . Since the values of σ_n are not as small in these cases, the contour levels are now at $\log_{10} |r_n^*(z)| = -1/3, -2/3, \dots$. Many of the 12 poles in each case lie outside these axes. Mathematically, these examples are not essentially different from those of Figures 1 and 2, since a Möbius transformation could reduce one type of topology to the other.

So far as we know, the optimal functions r_n^* in all these 14 example problems are unique (up to multiplication by a scalar of modulus 1). Note that the domains of Figures 1d, 1e, 1f, 2a, 2c, 3a, and 3d each have a line of symmetry, and those of Figures 1a, 1b, 2b, 3b, and 3c each have two lines of symmetry. The computed contour lines, poles, and zeros respect these symmetries quite well, with occasional deviations. Based on many experiments with various parameter choices, we believe that in each image, the value of σ_n displayed in the title is accurate to about two digits or more.

The images convey a vivid impression of electrostatic potential theory. It is known that the contour lines can be interpreted as level curves of the potential generated by positive logarithmic charges at each pole (i.e., of the form $\log |z - z_k|$) and negative ones at each zero, and the poles and zeros are positioned in such a way that the boundaries of E and F are approximate equipotential surfaces. For finite n , this interpretation gives bounds on σ_n , and as $n \rightarrow \infty$ it determines the exponential rate of decrease with n . This theory originates with Walsh [34], and for introductions, see [18, sec. 6] and [32, secs. 6–8].

The solutions plotted in Figures 1–3, while nearly optimal, need not be exactly so to plotting accuracy. In particular, the locations of the poles and zeros may not match those of the true optimal rational functions (which are only known analytically in rare cases involving a pair of intervals, a pair of disks, or a circular annulus [35]). In Figure 1a, for example, involving two disks of radius $1/2$ centered at ± 1 , the optimal

rational function is known to be a multiple of $[(z - \sqrt{3}/2)/(z + \sqrt{3}/2)]^{12}$, and the corresponding Zolotarev ratio is $\sigma_n = [(2 - \sqrt{3})/(2 + \sqrt{3})]^{12} \approx 1.8761 \times 10^{-14}$ [30]. This matches the computed value displayed in the figure, but the computed poles and zeros lie along small circles rather than coalescing at a point. Similarly in Figure 3a, where E is bounded by the circle of radius 0.5 about 0.2 and F by the unit circle, the exact solution would have a zero of order 12 at $1/a \approx 0.272$ and a pole of order 12 at $a \approx 3.68$ with $a = (79/40) + \sqrt{(79/40)^2 - 1}$ and $\sigma_n \approx 0.00047755$, again matching the computed value. Computationally, we find that the zeros are close to the predicted location but not quite confluent, and the poles, off these axes, lie approximately on a circle of radius ≈ 1 about the expected location. To numerical analysts these are instances of a familiar effect, that small changes in the values of a polynomial or rational function may be associated with large changes in its poles and zeros. To physicists or potential theorists, they are related to the phenomenon known in potential theory as *balayage*, going back to Poincaré or indeed one might say to Isaac Newton [15]. Outside the unit circle, for example, a uniform distribution of logarithmic charge on the circle generates the same potential as a point charge at the origin, and a finite collection of point charges uniformly spaced along the circle will approximate the same potential function exponentially closely.

2. The third and fourth Zolotarev problems. Yegor Ivanovich Zolotarev (1847–1878) was a student of Chebyshev who visited Berlin in 1872, where he learned about elliptic functions from lectures of Weierstrass. Back in St. Petersburg, he applied these methods to solve a collection of problems involving polynomial and rational functions posed on two real intervals [36]. Zolotarev died at age 31 after being hit by a train at the Tsarskoe Selo station, but his work lived on and was extended, among others, by Achieser in Kharkiv, Ukraine, who presented Zolotarev’s problems in his approximation theory and elliptic functions books [1, 2]. Later applications and generalizations were considered, among others, by Wachspress at the University of Tennessee [12], Gonchar and colleagues at the Steklov Institute in Moscow [14], Starke at the University of Karlsruhe [30], and Istace and Thiran at the University of Namur [17]. Our treatment here follows the presentation and notation of Istace and Thiran.

We have already stated the third Zolotarev problem Z3, whose general complex form is due to Gonchar [14]. For the fourth Zolotarev problem, whose complex generalization was introduced by Istace and Thiran, we first define the *sign function* relative to E and F :

$$(2.1) \quad \text{sign}_{E/F}(z) = \begin{cases} -1 & z \in E, \\ +1 & z \in F. \end{cases}$$

(For $z \in \mathbb{C} \setminus \{E \cup F\}$, $\text{sign}_{E/F}(z)$ is undefined.) Problem Z4, which might be called the *Zolotarev sign problem*, is the problem of rational minimax approximation of $\text{sign}_{E/F}$ over E and F :

Problem Z4 = Zolotarev sign problem. Find $\hat{r}_n \in R_n$ that attains the minimum

$$(2.2) \quad \tau_n = \min_r \|r - \text{sign}_{E/F}\|_{E \cup F},$$

where $\|\cdot\|_{E \cup F}$ denotes the supremum norm over $E \cup F$.

As usual with rational approximation, it is known that a solution exists, which satisfies $0 < \tau_n \leq 1$, but it need not be unique.

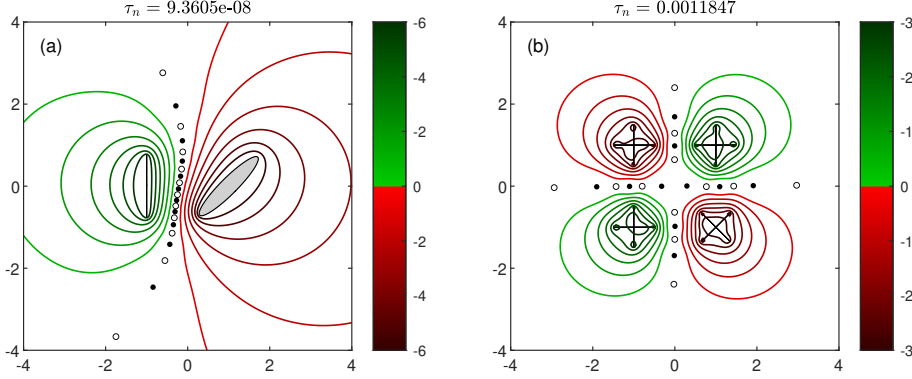


FIG. 4. Zeros (black circles) and poles (black dots) of the functions \hat{r}_n of Problem Z4 for the examples of Figures 1c and 2c, together with contour lines showing distances to +1 (red) and -1 (green). Specifically, on the left, the red contours show $\log_{10} |r_n(z) - 1| = -1, -2, \dots, -6$ and the green contours show $\log_{10} |r_n(z) + 1| = -1, -2, \dots, -6$; the pattern on the right is the same except with levels $-1/2, -1, -3/2, \dots, -3$. Images like this show that although Problem Z4 is posed just on the domains E and F , $\hat{r}_n(z)$ defines an approximation to a sign function throughout the complex plane, with its poles and zeros delineating an approximate branch cut. Computation of \hat{r}_n to solve Problem Z4 is the first step in our solution of Problem Z3.

In [2, p. 143], Achieser showed that problems Z3 and Z4 are equivalent in the case where E and F are real intervals. In [17], Istace and Thiran showed that the equivalence generalizes to the complex case. Here is their theorem, stated essentially in their words. The theorem is proved by a direct calculation, which we do not reproduce. In particular, it does not rely on characterizations of solutions to Problems Z3 or Z4.

THEOREM 2.1. *Every solution r_n^* of Problem Z3 is related to a solution \hat{r}_n of Problem Z4 by*

$$(2.3) \quad \hat{r}_n(z) = \frac{1 - \sigma_n}{1 + \sigma_n} \frac{r_n^*(z) - \sqrt{\sigma_n}}{r_n^*(z) + \sqrt{\sigma_n}}, \quad r_n^*(z) = \sqrt{\sigma_n} \frac{(1 - \sigma_n)/(1 + \sigma_n) + \hat{r}_n(z)}{(1 - \sigma_n)/(1 + \sigma_n) - \hat{r}_n(z)}.$$

The minimal values of the two problems satisfy

$$(2.4) \quad \tau_n = \frac{2\sqrt{\sigma_n}}{1 + \sigma_n}, \quad \sigma_n = \left(\frac{\tau_n}{1 + \sqrt{1 - \tau_n^2}} \right)^2,$$

and the set of extremal points

$$(2.5) \quad M = \{z \in E \cup F, |\hat{r}_n(z) - \text{sign}_{E/F}(z)| = \tau_n\}$$

is the union of $M_1 = \{z \in E, |r_n^*(z)| = \sigma_n\}$ and $M_2 = \{z \in F, |r_n^*(z)| = 1\}$.

Note that in the usual situation $\tau_n, \sigma_n \ll 1$, (2.3) and (2.4) reduce to

$$(2.6) \quad \hat{r}_n(z) \approx \frac{r_n^*(z) - \sqrt{\sigma_n}}{r_n^*(z) + \sqrt{\sigma_n}}, \quad r_n^*(z) \approx \frac{\tau_n}{2} \frac{1 + \hat{r}_n(z)}{1 - \hat{r}_n(z)}$$

and

$$(2.7) \quad \tau_n \approx 2\sqrt{\sigma_n}, \quad \sigma_n \approx \frac{\tau_n^2}{4}.$$

The factor $\tau_n/2$ in (2.6) is just the scaling (1.2), so the essential point is that rational functions with small ratios (1.1) come from approximations $\hat{r}_n(z) \approx \text{sign}_{E/F}(z)$ via $(1 + \hat{r}_n)/(1 - \hat{r}_n)$.

As we will discuss in the next section, our algorithm for solving Problem Z3 consists of solving Problem Z4 and then transforming from \hat{r}_n and τ_n to r_n^* and σ_n . To give an idea of the mathematics of the equivalence, Figure 4 shows the poles and zeros of the functions \hat{r}_n for the examples of Figures 1c and 2c, which line up along curves approximating branch cuts for $\text{sign}_{E/F}$. The contour lines show distances to 1 (red) and -1 (green).

3. Numerical method. AAA approximation produces a rational function represented in barycentric form. In the notation of [23, eq. (3.2)], we have

$$(3.1) \quad r(z) = \sum_{k=0}^n \frac{\alpha_k}{z - t_k} \bigg/ \sum_{k=0}^n \frac{\beta_k}{z - t_k},$$

where t_0, \dots, t_n are *support points* and $\alpha_0, \dots, \alpha_n$ and β_0, \dots, β_n are *barycentric weights*. Note that $\{t_k\}$ are not poles of r (assuming the weights are nonzero), but points where the quotient takes the limiting values $\{\alpha_k/\beta_k\}$. The zeros and poles of r are the zeros of the numerator and denominator of (3.1), respectively, which can be calculated accurately by means of a matrix generalized eigenvalue problem [22, eq. (3.11)].

Mathematically, any choice of support points $\{t_k\}$ in (3.1) would do, but the power of the barycentric representation lies in its exceptional numerical stability when the support points are selected in a manner fitted to the function being represented, as is accomplished by the AAA algorithm.

Following Theorem 2.1, we solve Problem Z3 in two steps:

- (1) *Solve Problem Z4 by AAA-Lawson approximation with Chebfun `aaa.m`;*
- (2) *Convert to a solution of Problem Z3 by (2.3) and (2.4).*

Step (2) is straightforward, so we just make one comment on this before turning to discuss the more challenging step (1). By (2.3), the zeros and poles of r_n^* are the points z where $\hat{r}_n = -p$ and $+p$, respectively, where $p = (1 - \sigma_n)/(1 + \sigma_n)$. To compute these numbers, we take the barycentric data $\{t_k\}$, $\{\alpha_k\}$, $\{\beta_k\}$ defining \hat{r}_n and simply subtract or add $p\beta_k$ to each α_k . Thus \hat{r}_n is decreased or increased by p at each support point, hence by the same constant at all $z \in \mathbb{C}$ since the values at these points determine a degree n rational interpolant. To find the zeros and poles of r_n^* , it remains only to perform zerofinding on the barycentric representations of $\hat{r}_n \pm p$ in the usual way via generalized eigenvalue problems.

This brings us to the main challenge of our algorithm, step (1) above, the computation of the degree n rational best approximation \hat{r}_n to the sign function $\text{sign}_{E/F}$ defined by the sets E and F . The high-level summary is that we find \hat{r}_n by AAA approximation, which is a fast and robust algorithm for computing near-best rational approximations [8, 22]. However, this has proved not as straightforward as one would expect. Two difficulties arise, and it is because of these that we were unable to write a paper like the present one a few years ago, when AAA first became available. The first difficulty is that AAA encounters particular challenges when applied to sign functions, which has not been noticed before. The second is that for clean Zolotarev results, it is important to have not just good rational approximations but nearly optimal ones, requiring the use of the AAA-Lawson algorithm [23], which had a known problem of non-convergence in certain cases that we have also had to address.

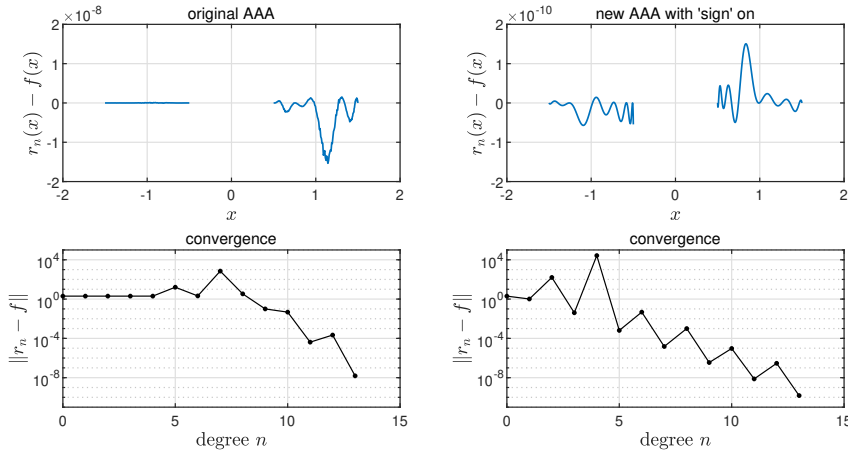


FIG. 5. AAA convergence for degree $n = 13$ approximation $\hat{r}_n \approx \text{sign}_{E/F}$ with $E = [-1.5, -0.5]$ and $F = [0.5, 1.5]$, with each interval approximated by 200 Chebyshev points. On the left, the original AAA iteration reveals difficulties typical of many $\text{sign}_{E/F}$ examples. The “blending of singular values” adjustment described in the text produces the better results on the right. (This would then further improve to an equioscillatory error curve with the AAA-Lawson iteration with damping, as illustrated for a more difficult problem in Figure 6.) The sawtoothed convergence curve reflects poles falling between sample points at every other iteration, a common phenomenon in approximation of even or odd functions on real domains.

We will discuss these difficulties, and what we have done about them, in two subsections.

3.1. Modification of AAA for sign functions. The AAA algorithm has not changed fundamentally since its appearance in 2018 [22]. Although it has no guarantee of convergence, we tend to think of it as “99% reliable,” at least when used with dense enough sample grids and error tolerances well above the level of noise. For a wide range of problems, it reliably produces near-best rational approximations, typically with errors about a factor of ten above the true minima.

Experiments in approximation of functions of the form $\text{sign}_{E/F}$, however, give unsatisfactory results. The left column of Figure 5 illustrates what tends to happen. The initial iterations achieve nothing, and at the end, the error curve is very irregular and far from optimal. After much experimentation we have discovered the part of the algorithm that causes the trouble. As described around eq. (3.5) of [22], AAA computes a singular value decomposition (SVD) at each step to determine a minimal singular vector defining barycentric weights to solve a least-squares problem. The trouble is that in certain cases, the minimal singular value with standard AAA is degenerate or nearly so, and this is associated with a singular vector containing zeros or near-zeros in certain entries. To fix this, we have introduced a new option essentially to replace the MATLAB lines

```
[~,S,V] = svd(A(J,:),0);
wj = V(:,end);
```

by the alternative

```
[~,S,V] = svd(A(J,:),0);
s = diag(S); wj = V*(1./s.^2); wj = wj/norm(wj);
```

This has the effect that a certain barycentric weight vector \mathbf{w}_j , rather than being

formed from a single minimal singular vector, is computed as a blend of all the singular vectors with strong bias towards the minimum. The effect on most AAA computations appears to be negligible, but for certain problems such as approximation of sign functions, there is a real improvement, as suggested in the right column of Figure 5. Note the vertical scales.

In the Chebfun AAA code `aaa.m`, this modification was introduced as an option in July 2024 specified by an optional flag `'sign'`, which we have invoked for all the computations of this paper.

3.2. Modification of Lawson iteration to enhance robustness. To improve rational approximations from near-best to best, the standard method is AAA-Lawson iteration. As described in section 3 of [23], this is a nonlinear variant of iteratively reweighted least-squares which often converges to minimax approximations, recognizable by their equioscillatory error curves in real cases and nearly-circular error curves in complex problems. The centerpiece of the Lawson iteration is an adjustment of the weights in a least-squares problem (linear) according to the errors at the same points in the current rational approximation (nonlinear). This is given as eq. (3.7) of [23],

$$(3.2) \quad w_j^{(\text{new})} = w_j |e_j|,$$

where w_j denotes the current least-squares weight at sample point z_j and e_j is the current rational approximation error $e_j = r(z_j) - f_j$. (Note that these least-squares weights, which belong to the hundreds or thousands of sample points of the grid, have nothing to do with the barycentric weights discussed earlier, which belong just to the subset of $n + 1$ barycentric support points.) In successful cases, iterating (3.2) leads to linear convergence to a weighted least-squares solution that is equal to the minimax approximation being sought. Such convergence has long been known to be guaranteed for the Lawson iteration applied to linear problems, but with AAA-Lawson, the iteration is nonlinear and there is no guarantee.

Unfortunately, unlike ordinary AAA iteration, AAA-Lawson has always been “just 90% reliable.” It fails rather often, and when it fails, as illustrated in Figure 6.1 of [23], the failure often takes the form of a period-2 oscillation, showing high errors on the left of a domain at one Lawson step and then high errors on the right of the domain at the next step. We have found that these troubles show up quite often with approximation of $\text{sign}_{E/F}$ functions. Zolotarev problems appear to lie in an exceptionally problematic regime of AAA approximation.

We have investigated this problem and developed a modified algorithm that often improves matters. The idea is to replace (3.2) by a modified weight update formula

$$(3.3) \quad w_j^{(\text{new})} = \left((1 - \delta) + \frac{\delta |e_j|}{\max_j |e_j|} \right) w_j,$$

where $\delta \in (0, 1]$ is a damping factor. If $\delta = 1$ we have standard AAA-Lawson, whereas for smaller values we have a more robust iteration that is more likely to converge. In August 2024 this modification was introduced as an option in Chebfun `aaa.m` specified by a flag `'damping'` followed by the number δ . Figure 6 gives two illustrations of the improved convergence of certain iterations with damping. For the Zolotarev computations of this paper we have taken $\delta = 0.95$; details for each example problem are given in the appendix.

In two subsections, we have presented two modifications of the AAA algorithm that make it more effective in approximating the $\text{sign}_{E/F}$ functions arising in Zolotarev

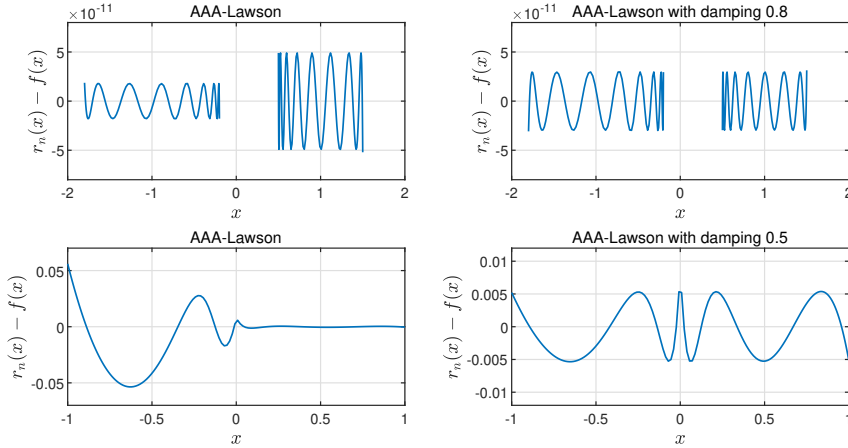


FIG. 6. *First row: AAA convergence for degree 15 approximation of $\text{sign}_{E/F}$ with $E = [-1.8, -0.2]$ and $F = [0.5, 1.5]$, with each interval approximated by 100 Chebyshev points. On the left, the result of AAA followed by 150 steps of AAA-Lawson iteration. On the right, the same but with AAA-Lawson applied with damping factor $\delta = 0.8$. Second row: a similar comparison for degree $n = 4$ rational approximation of $\text{ReLU}(x) = \max(x, 0)$, sampled in 200 Chebyshev points, with damping factor $\delta = 0.5$.*

problems. We do not regard either of these adjustments as a definitive solution. AAA and AAA-Lawson still give suboptimal results on certain problems, and we hope that further investigation will lead to further improvements. Ideally one would like algorithms requiring no human intervention such as the specification of a damping factor δ , and one would like to have a proof that they always converge. AAA and AAA-Lawson continue to advance, but we are a long way from this state.

Using Chebfun `aaa` and `prz` syntax as of August 2024, the functions \hat{r}_n and r_n^* for the example of Figure 1a can be computed by this code segment in about 0.3 s on our laptop. The code writes q for \hat{r}_n and r for r_n^* .

```

np = 400; cc = exp(2i*pi*(1:np)'/np);
E = -1 + .5*cc; F = 1 + .5*cc;
fEF = [-ones(size(E)); ones(size(F))];
[q,qpoles,~,qzeros,zj,fj,wj] = aaa(fEF,[E;F], ...
    'degree',12,'sign',1,'lawson',200,'damping',0.9);
tau = norm(fEF-q([E;F]),inf)
sigma = (tau/(1+sqrt(1-tau^2)))^2
p = (1-sigma)/(1+sigma);
r = @(z) sqrt(sigma)*(p+q(z))./(p-q(z));
[~,~,rpoles] = prz(zj,fj+p,wj);
[~,~,rzeros] = prz(zj,fj-p,wj);

```

To give a further indication of the behavior of our methods, Figure 7 shows computed σ_n as a function of $n = 0, 1, \dots, 70$ for a difficult problem involving a pair of rectangles, as shown in the inset of the figure. The outer corners lie at $\pm 1 \pm i$, and the inner corners at $\pm 1/4 \pm i$, and we took 200 AAA-Lawson steps with damping parameter 0.95. This kind of configuration has been studied in the past, though without a numerical method available to calculate Zolotarev rational functions directly [26, 35]. Because of the higher degrees involved, this computation took about a minute on our laptop. The numerical values come close to the lower bound for the Zolotarev ratio

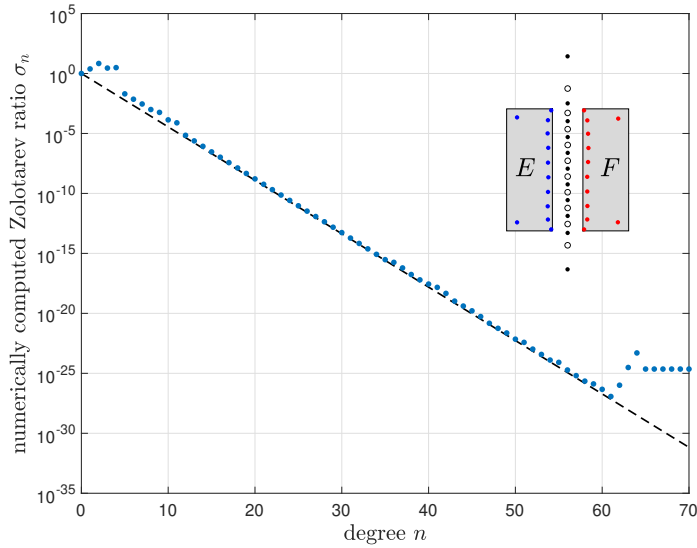


FIG. 7. Decrease of numerically computed σ_n as a function of n for a problem where E and F are a pair of rectangles. The inset shows the geometry together with the poles (red) and zeros (blue) of r_n^* and the poles (black dots) and zeros (black circles) of \hat{r}_n for the case $n = 12$. The dashed line shows the lower bound (3.4) from potential theory. The data points for $n = 1, 2, 3, 4$ are obviously inaccurate, and we suspect all the values for $1 \leq n \leq 11$ should lie closer to the lower bound.

that can be derived from potential theory via numerical conformal mapping,

$$(3.4) \quad \sigma_n \geq h^{-n} = e^{-n/\text{cap}(E,F)}$$

where $\text{cap}(E, F)$ is what is known as the *condenser capacity* of the pair E, F [18]. We computed the capacity $\text{cap}(E, F) \approx 2.78805$ by methods of rational approximation [31], reflecting the curious situation that in the end, approximate estimates for Zolotarev numbers are not always simpler to calculate than the Zolotarev numbers themselves.

4. Applications of the Zolotarev ratio problem Z3. The most famous application of the Zolotarev ratio problem Z3 is to ADI-related matrix iterations in numerical linear algebra. To explain, we begin with the more basic case of polynomial iterations.

Suppose we want to solve

$$(4.1) \quad Cx = y,$$

where C is a square matrix, y is a vector, and x is an unknown vector. Existence of a unique solution is guaranteed if C is nonsingular. Many matrix iterations generate sequences x_0, x_1, \dots with error vectors $e_k = C^{-1}y - x_k$ satisfying

$$(4.2) \quad e_k = p_k(C)e_0,$$

where p_k is a polynomial of degree k with $p(0) = 1$ [9]. In particular this is true of the Chebyshev, Richardson, conjugate gradient, MINRES, and GMRES iterations [13, 27]. Equation (4.2) then implies

$$(4.3) \quad \frac{\|e_k\|}{\|e_0\|} \leq \|p_k(C)\|,$$

where $\|\cdot\|$ is any norm. If $\|\cdot\|$ is the 2-norm and $\Lambda(C)$ is the spectrum of C , i.e. its set of eigenvalues, then (4.3) implies

$$(4.4) \quad \frac{\|e_k\|}{\|e_0\|} \leq \|p_k\|_\Lambda,$$

where $\|p_k\|_\Lambda = \max_{z \in \Lambda} |p_k(z)|$, assuming C is normal (e.g. real symmetric or complex hermitian). If C is nonnormal, then among various possible generalization of (4.4) we have

$$(4.5) \quad \frac{\|e_k\|}{\|e_0\|} \leq \kappa(V) \|p_k\|_\Lambda,$$

where $\kappa(V)$ is the 2-norm condition number of any matrix V of eigenvectors of C , assuming one exists.

Equations (4.1)–(4.5) tell us that rapid convergence of an iteration is guaranteed if it corresponds to a sequence of polynomials p_0, p_1, \dots normalized by $p_k(0) = 1$ that converge quickly to 0 on Λ . This connection between polynomial approximation and matrix iterations has been known and exploited since the 1950s.

Rational approximations enter the picture when we generalize (4.1) to the *Sylvester equation*,

$$(4.6) \quad AX - XB = Y,$$

where A is an $m \times m$ matrix, B is an $n \times n$ matrix, Y is an $m \times n$ matrix, and X is an unknown $m \times n$ matrix. (The special case with $A = -B^*$ and $Y = Y^*$ is called the *Lyapunov equation*.) These equations arise in many applications, from reduced order modeling and signal processing to the solution of PDEs. See [28] and references therein. Existence of a unique solution is guaranteed if the spectra of A and B are disjoint. At first glance (4.6) may look like a very different problem from (4.1), and rather niche, but in fact, (4.1) takes the form (4.6) in important cases where the matrix C has special structure. This observation became famous with the introduction of *Alternating Direction Implicit* or *ADI* iteration by Peaceman and Rachford in 1955 [25]. In their original model problem, X corresponds to the unknown values of a discretized finite difference solution to a two-dimensional linear PDE on an $m \times n$ grid, and the matrices A and B are finite difference operators with respect to the two different directions. Peaceman and Rachford discovered that (4.6) could be solved very efficiently by an iteration in which one applied $(A - \beta_j I_n)^{-1}$ on the left and $(B - \alpha_j I_m)^{-1}$ on the right at alternate steps, both involving easy tridiagonal linear solves, for appropriate constants α_j and β_j , known as *shift parameters*. Omitting details, which can be found for example in [28] and [35], this leads to an iterative sequence X_0, X_1, \dots with error matrices $E_k = X - X_k$ satisfying

$$(4.7) \quad E_k = r_k(A) E_0 r_k(B)^{-1},$$

where r_k is the degree k rational function

$$(4.8) \quad r_k(z) = \prod_{j=1}^k \frac{z - \alpha_j}{z - \beta_j}.$$

In analogy to (4.4), this implies

$$(4.9) \quad \frac{\|E_k\|}{\|E_0\|} \leq \frac{\max_{z \in \Lambda_A} |r(z)|}{\min_{z \in \Lambda_B} |r(z)|}$$

if A and B are normal, with appropriate extensions in the nonnormal case. And here we recognize the Zolotarev ratio problem of (1.1). Thus we see that the numerical method proposed in this paper offers a new tool for design and analysis of ADI iterations.

Beyond the basics just outlined, there have been a number of further applications of the Zolotarev ratio problem in numerical linear algebra. One area of application is to rational Krylov and related methods [5, 10]. Another, investigated recently by Beckermann and Townsend [6], concerns the case where the solution matrix X of (4.6) is of large dimension but of low *numerical rank*, meaning that its singular values decay rapidly. Theorem 2.1 of [6] shows that if A and B are normal and Y is of rank $\nu \geq 1$ in (4.6), then for each k , the singular value of X of index $1 + \nu k$ of X can be bounded in terms of the Zolotarev ratio σ_k of (1.3), where E and F are any sets containing the spectra of A and B . Thus when Y is of low rank, X is guaranteed to be of small numerical rank, with singular values decaying at an exponential rate determined by the Zolotarev problem. The tools introduced in the present paper should make it possible to explore this phenomenon in much more general cases than have been accessible before.

5. Applications of the Zolotarev sign problem Z4. As well as being a step toward the solution of Z3, problem Z4 is also of interest in its own right. Problems of this kind arise in many contexts where one wants to separate one part of a system computationally from another. For example, the 1970s introduced the major technology of digital signal processing. A “recursive” or “infinite impulse response” low-pass, high-pass, or band-pass filter starts from a rational function that is nearly constant on one part of the real axis and nearly zero on another, and finding such a function is essentially a Zolotarev sign problem [24].

Generalizations, as usual, come from numerical linear algebra and its applications in computational science. For computing eigenvalues of large matrices, one of the classes of available methods is *divide and conquer* algorithms, where one part of the spectrum is suppressed relative to another in a possibly recursive fashion [3, 4]. This leads quickly to Zolotarev sign problems, typically starting from the case where E and F are approximations to the left and right complex half-planes [21]. In the real case, which goes back to Zolotarev himself, they may be intervals such as $[-a, -\varepsilon]$ and $[\varepsilon, a]$. “Spectral slicing” ideas of this kind have found wide generalization through algorithms such as FEAST, with applications for example in electronic structure calculation in physics [16, 19]. Here an approximate sign function is used to isolate a region of the complex plane containing eigenvalues of mathematical or physical interest. Mathematically, the issue is the numerical projection of a large space of functions onto an interesting smaller-dimensional subspace.

Wherever approximate sign functions are in play, so are rational approximations to branch cuts, which in turn are close to numerical quadrature formulas. Our numerical method for Problem Z4 can be applied to the derivation of new (and old) quadrature formulas, a topic to be investigated in a later paper.

6. Discussion. Before the current contribution, methods for computing Zolotarev functions were not available, but various types of approximations have been discussed in the literature. We mentioned the lower bound (3.4) in connection with Figure 7, and to derive upper bounds together with approximate Zolotarev functions, one can use Faber rational functions [26] or Walsh–Fejer, Leja, or generalized Leja points on the boundary [11, 29]. All these estimates require some work to apply, however, to solve associated conformal mapping or optimization problems.

The algorithm we have proposed is not yet bulletproof. Further improvements in Zolotarev computations will probably be associated with further improvements in the AAA and AAA-Lawson algorithms, which we hope will be stimulated by the discussion here especially in section 3. For the moment, we have relied on the Chebfun implementation of AAA in MATLAB/Octave, which includes the 'sign' and 'damping' improvements we have discussed [8]. Implementations of AAA are available in other languages, including Julia [7, 20] and Python via the SciPy package (release 1.15.0, January 2025, code written by Jake Bowhay) [33]. At present these lack 'sign' and 'damping', so they may give less accurate results for Zolotarev problems than what we have shown here. Of course, software changes rapidly, and the details of available options will surely be different in a few years. What will remain is that approximation algorithms have now advanced to the point where Zolotarev rational functions can be computed numerically.

Acknowledgments. We have benefited from helpful comments from Bernard Beckermann, Nick Hale, and Yuji Nakatsukasa. Nakatsukasa in particular contributed to the algorithmic improvements in AAA described in section 3.

Appendix. Details of computed examples. For all the examples of Figures 1–3, we ran AAA with 'sign' on followed by AAA-Lawson iteration with damping factor 0.95; the number of iterations was 200 in Fig. 1 and 400 in Figs. 2 and 3. In the following descriptions of the approximation sets E and F , S denotes the set of 200 roots of unity, i.e., 200 equispaced points on the unit circle.

Specifications for Figure 1. (a) Circles $\pm 1 + 0.5S$. (b) Intervals $[-1.5, -0.5]$ and $[0.5, 1.5]$, each discretized by 200 Chebyshev points. (c) On the left, 200 Chebyshev points in the interval $[-1 - 0.75i, -1 + 0.75i]$, and on the right, the ellipse $1 + (0.2\text{Re}(S) + i\text{Im}(S))/\sqrt{i}$. (d) Let T be the semicircle consisting of the 101 points of S in the right half-plane. The yin figure is composed of three copies of T , two of them reduced to half-size, and all shifted left by 0.5, and the yang is the negative of the yin. (e) On the right, the semicircle $1 - 0.74T$, and on the left, three sides of a square of side length 0.75 centered at -1 , each side discretized by 100 Chebyshev points. (f) 200 Chebyshev points in $[1, 2]$ together with $(-\infty, 0]$ discretized by 200 exponentially graded points: `Matlab 1-logspace(0,5,200)`.

Specifications for Figure 2. (a) Circles $-1 + 0.5S$ and $0.8 + 0.3S \pm 0.6i$. (b) The intervals $[-2, -1]$ $[-0.5, 0.5]$, and $[1, 2]$, each discretized by 100 Chebyshev points. (c) If X is the cross composed of 100 Chebyshev points in $[-0.5, 0.5]$ and 100 Chebyshev points in $[-0.5i, 0.5i]$, the sets are composed from $X \pm 1 \pm i$, with the lower-right cross rotated by $\pi/4$. (d) Six equilateral triangles scaled to circles of radius 0.5. On the right, the triangles are centered at 1 and $1 \pm i$, and on the left, they are rotated by $\pi/6$ and positioned with centers at correspondingly transformed positions -1 and $-1 \pm i \mp 1/\sqrt{3}$.

Specifications for Figure 3. (a) Circles S and $0.2 + 0.5S$. (b) Outside, the ellipse obtained by stretching S by a factor 1.5 along the x axis, and inside, the square of side length 1, each side discretized by 100 Chebyshev points, rotated by angle $\pi/8$. (c) Circle S and the ellipse $\exp(0.2i)(0.4\text{Re}(S) + 0.7i\text{Im}(S))$. (d) Circle S and the two smaller circles $0.1 \pm 0.5i + 0.3S$.

Specifications for Figure 7. The rectangles are discretized by 50 Chebyshev points on the ends and 100 points on the sides.

REFERENCES

- [1] N. I. ACHIESER, *Theory of Approximation*, Ungar, New York, 1956.
- [2] N. I. AKHIEZER, *Elements of the Theory of Elliptic Functions*, Amer. Math. Soc., Providence, RI, 1990.
- [3] Z. BAI, J. DEMMEL, AND M. GU, *An inverse free parallel spectral divide and conquer algorithm for nonhermitian eigenproblems*, Numer. Math., 76 (1997), pp. 279–308.
- [4] J. BANKS, J. GARZA-VARGAS, A. KULKARNI, AND N. SRIVASTAVA, *Pseudospectral shattering, the sign function, and diagonalization in nearly matrix multiplication time*, Found. Comp. Math., 23 (2023), pp. 1959–2047.
- [5] B. BECKERMANN, *An error analysis for rational Galerkin projection applied to the Sylvester equation*, SIAM J. Numer. Anal., 49 (2011), pp. 2430–2450.
- [6] B. BECKERMANN AND A. TOWNSEND, *Bounds on the singular values of matrices with displacement structure*, SIAM Rev., 61 (2019), pp. 319–344.
- [7] T. A. DRISCOLL, *RationalFunctionApproximation.jl: Julia software for approximation by rational functions*, <https://github.com/complexvariables/RationalFunctionApproximation.jl>, 2023. DOI: zenodo.org/records/8355791.
- [8] T. A. DRISCOLL, N. HALE, AND L. N. TREFETHEN, EDS., *Chebfun User’s Guide*, Pafnuty Publications, Oxford, UK, 2014. See also <http://www.chebfun.org>.
- [9] T. A. DRISCOLL, K.-C. TOH, AND L. N. TREFETHEN, *From potential theory to matrix iterations in six steps*, SIAM Rev., 40 (1998), pp. 547–578.
- [10] V. DRUSKIN, L. KNIZHNERMAN, AND V. SIMONCINI, *Analysis of the rational Krylov subspace and ADI methods for solving the Lyapunov equation*, SIAM J. Numer. Anal., 49 (2011), pp. 1875–1898.
- [11] V. DRUSKIN AND V. SIMONCINI, *Adaptive rational Krylov subspaces for large-scale dynamical systems*, Systems & Control Letters, 60 (2011), pp. 546–560.
- [12] N. S. ELLNER AND E. L. WACHSPRESS, *Alternating direction implicit iteration for systems with complex spectra*, SIAM J. Numer. Anal., 28 (1991), pp. 859–870.
- [13] G. H. GOLUB AND C. F. VAN LOAN, *Matrix Computations*, JHU Press, 2013.
- [14] A. A. GONCHAR, *Zolotarev problems connected with rational functions*, Math. USSR-Sb., 7 (1969), pp. 623–635.
- [15] B. GUSTAFSSON, *Lectures on Balayage*, U. of Joensuu, Dept. Rep. Ser., 2001.
- [16] S. GÜTTEL, E. POLIZZI, P. T. P. TANG, AND G. VIAUD, *Zolotarev quadrature rules and load balancing for the FEAST eigensolver*, SIAM J. Sci. Comp., 37 (2015), pp. A2100–A2122.
- [17] M.-P. ISTACE AND J.-P. THIRAN, *On the third and fourth Zolotarev problems in the complex plane*, SIAM J. Numer. Anal., 32 (1995), pp. 249–259.
- [18] E. LEVIN AND E. B. SAFF, *Potential theoretic tools in polynomial and rational approximation*, in J.-D. Fournier, et al. (eds.), Harmonic Analysis and Rational Approximation, v. 3, Springer, New York (2006), pp. 71–94.
- [19] L. LIN, J. LU, AND L. YING, *Numerical methods for Kohn–Sham density functional theory*, Acta Numer., 28 (2019), pp. 405–539.
- [20] D. MACMILLEN, *BaryRational.jl*, github.com/macd/BaryRational.jl, 2024.
- [21] Y. NAKATSUKASA AND R. W. FREUND, *Computing Fundamental matrix decompositions accurately via the matrix sign function in two iterations: the power of Zolotarev’s functions*, SIAM Rev., 58 (2016), pp. 461–493.
- [22] Y. NAKATSUKASA, O. SÈTE, AND L. N. TREFETHEN, *The AAA algorithm for rational approximation*, SIAM J. Sci. Comput., 40 (2018), pp. A1494–A1522.
- [23] Y. NAKATSUKASA AND L. N. TREFETHEN, *An algorithm for real and complex rational minimax approximation*, SIAM J. Sci. Comput., 42 (2020), pp. A3157–A3179.
- [24] A. V. OPPENHEIM AND R. W. SCHAFER, *Discrete-Time Signal Processing*, Pearson, 2001.
- [25] D. W. PEACEMAN AND H. H. RACHFORD, JR., *The numerical solution of parabolic and elliptic differential equations*, J. SIAM, 3 (1955), pp. 28–41.
- [26] D. RUBIN, A. TOWNSEND, AND H. WILBER, *Bounding Zolotarev numbers using Faber rational functions*, Constr. Approx., 56 (2022), pp. 207–232.
- [27] Y. SAAD, *Iterative Methods for Sparse Linear Systems*, SIAM, 2003.
- [28] V. SIMONCINI, *Computational methods for linear matrix equations*, SIAM Rev., 58 (2016), pp. 377–441.
- [29] G. STARKE, *Optimal alternating direction implicit parameters for nonsymmetric systems of linear equations*, SIAM J. Numer. Anal., 28 (1991), pp. 1431–1445.
- [30] G. STARKE, *Near-circularity for the rational Zolotarev problem in the complex plane*, J. Approx. Theory, 70 (1992), pp. 115–130.
- [31] L. N. TREFETHEN, *Numerical conformal mapping with rational functions*, Comput. Methods

- and Function Theory, 20 (2020), pp. 369–387.
- [32] L. N. TREFETHEN, *Numerical analytic continuation*, Japan J. Appl. Math., 40 (2023), pp. 1587–1636.
 - [33] P. VIRTANEN, ET AL., *SciPy 1.0: fundamental algorithms for scientific computing in Python*, Nature Methods, 17 (2020), pp. 261–272.
 - [34] J. L. WALSH, *Interpolation and Approximation by Polynomials and Rational Functions in the Complex Domain*, 5th ed., Amer. Math. Soc., 1969.
 - [35] H. D. WILBER, *Computing Numerically with Rational Functions*, PhD thesis, Dept. of Mathematics, Cornell U., 2021.
 - [36] E. ZOLOTAREV, *Application of elliptic functions to questions of functions deviating least and most from zero*, Zap. Imp. Akad. Nauk. St. Petersburg, 30 (1877), pp. 1–59 [Russian].